VOLUME 80 SEPARATE No. 480

PROCEEDINGS

AMERICAN SOCIETY OF CIVIL ENGINEERS

AUGUST, 1954

AMERICAN SOCIETY OF CIVIL ENGINEERS FOUNDED 1852

DISCUSSION OF PROCEEDINGS - SEPARATES

182, 198, 201, 245, 291

STRUCTURAL DIVISION

Headquarters of the Society
33 W. 39th St.
New York 18, N. Y.

PRICE $0.50 PER COPY

Current discussion of papers sponsored by the Structural Division is presented as follows:

This paper was published at 1745 S. State Street, Ann Arbor, Mich., by the American Society of Civil Engineers. Editorial and General Offices are at 33 West Thirty-ninth Street, New York 18, N.Y.

DISCUSSION OF HIPPED PLATE ANALYSIS, CONSIDERING JOINT DISPLACEMENT PROCEEDINGS-SEPARATE NO. 182

Herman Craemer.[12]—Following World War II hipped plate design was

[12] Civ. Engr., Germany.

once again undertaken after it had been ignored for fifteen years preceding the war. Many investigations, valuable and otherwise have been conducted. Mr. Gaafar is to be congratulated for his valuable contribution to the field.

During the investigations conducted by Mr. Ehlers[3] and the writer,[5, 6, 8]

[3] "Ein neues Konstruktionprinzip," by G. Ehlers, *Bauingenieur*, Vol. 9, 1930, p. 125.
[5] "Der heutige Stand der Theorie der Scheibentraeger und Faltwerke, in Eisenbeton," by H. Craemer, *Beton und Eisen*, Vol. 36, 1937, p. 264.
[6] *Ibid.*, p. 297.
[8] "Theorie der Faltwerke," by H. Craemer, *Beton und Eisen*, Vol. 29, 1930, p. 276.

the effect of the deflection of the edges was greatly underrated. Mr. Gaafar's statements (under the heading, "Introduction—Previous Theory") that "* * * the plates were assumed to be connected by hinged joints" and that the connecting moments of the slabs along the edges were "neglected entirely" were erroneous, however, because it was clearly stated (by Mr. Ehlers and the writer) that in the direction normal to the edges, the system behaves like a continuous slab rigidly supported at the edges. Thus, the oversimplification does not consist in neglecting the continuity but only in neglecting the translation of the edges. The comparison of the "approximate theory" with Mr. Gaafar's approach is therefore somewhat misleading.

The writer has conducted an investigation[13] which is based on the same

[13] "Design of Prismatic Shells," by H. Craemer, *Journal*, A. C. I., No. 6, February, 1953.

assumptions listed under the heading "Limitations." It was found that the behavior of the system depends on the stiffness coefficient,

$$c = \frac{K\, t^2\, L^4}{h^6} \qquad (9)$$

in which K is a function of the shape of the cross section and the distribution of a load across the latter. If $c = 0$, the writer's elementary theory—but not the "approximate theory" in Mr. Gaafar's meaning—is correct. If c is infinite, the cross section as a whole behaves like an ordinary beam with a linear distribution of the longitudinal stresses. Thus, there is a gradual transition from "pure shell effect" ($c = 0$) to "pure beam effect" ($c = \infty$).

Although the writer's work[13] is probably easier to understand than the papers by Mr. Gruber,[4, 7] it is necessarily more complex than Mr. Gaafar's

[4] "Berechnung prismatischer Scheibenwerke," by E. Gruber, *Memoirs*, International Assn. of Bridge and Structural Eng., Vol. 1, 1932, p. 225.
[7] "Die Berechnung pyramidenartiger Scheibenwerke und ihre Anwendung auf Kaminkuehler," by E. Gruber, *Memoirs*, International Assn. of Bridge and Structural Eng., Vol. 2, 1933–1934, p. 206.

work because the writer's investigation takes into consideration the geometrical compatibility along the whole length of edges, thus leading to differential equations.

One of the author's principal simplifying statements is that the edge-translations are sinusoidal. However, since the transverse moments depend linearly on the latter, the transverse moments should also be sine waves. For a system

approximating pure beam effect, however, this is not correct. This case is similar to the case of a narrow rectangular slab supported at the four edges and subjected to a uniform load, within which the moments in the direction of the short span are sensibly constant except near the short edges. This cannot be described by one sine wave. There is too much interaction in a prismatic shell between the various statical and geometrical effects occurring at a number of edges to allow for a simple approach covering the whole range of stiffness coefficients. Mr. Gaafar's work may nonetheless be useful for systems that approximate the pure shell effect.

For large values of c, a first approximation might be the assumption of pure beam effect; to this condition corrections to fulfill the geometrical conditions might be applied. There is a great need for theoretical research in hipped plate design and analysis.

James M. Paulson,[14] J. M. ASCE, and L. C. Maugh,[15] M. ASCE.—This paper provides much valuable information concerning the analysis of hipped plate or prismatic roof structures which consist of an assemblage of plate elements rigidly connected at their edges. Mr. Gaafar asserts (and it is substantiated by model tests) that both the transverse and longitudinal stresses are influenced considerably by the components of the edge displacements normal to the planes of the various plate elements. As the analysis is greatly complicated by this distortion of the cross section, it is of importance to determine whether such displacements need be considered when uniformly distributed forces only are acting. This problem had been investigated by Mr. Craemer,[13] although the arrangement of the material and procedure is quite different from that given by the author. Mr. Craemer was concerned more with the deviation from the linear distribution of the longitudinal stresses (as given by the ordinary beam formula) than with the discrepancies in the approximate hipped plate theory. Mr. Gaafar has noted that this theory does not consider the effect of edge displacements.

[14] Asst. Prof. in Civ. Eng., Wayne Univ., Detroit, Mich.
[15] Prof. of Civ. Eng., Univ. of Michigan, Ann Arbor, Mich.

The writers have evaluated the error in the results obtained by the approximate method for structures of various proportions when subjected to a uniformly distributed vertical load. In Table 10 a comparison is shown of the correction s_c of the longitudinal stress caused by edge displacements to the

TABLE 10.—Value of the Ratio s_c/s_a at the Edges of the Edge Beams

Edge-beam depth, in feet	Width-to-Length Ratio					
	0.288		0.407		0.576	
	Top edge	Bottom edge	Top edge	Bottom edge	Top edge	Bottom edge
7.5	+0.034	−0.028	+0.0092	−0.0076	+0.0023	−0.0019
3.75	+0.36	−0.19	+0.12	−0.062	+0.029	−0.015
1.875	+4.52	−0.56	+2.23	−0.29	+0.83	−0.098
0.9375	−3.43	−0.87	−2.80	−0.71	−1.60	−0.41

stress s_a which is obtained by the approximate method in terms of the ratio s_c/s_a. The term s_c is the difference in the longitudinal stress between the approximate method and Mr. Gaafar's solution which considers edge displacements. The values given in Table 10 are for a structure similar to the hipped plate roof shown in Fig. 2. Such a structure is designated as a "three-segment roof." Table 10 shows the variation in s_c/s_a at the top and bottom edges for various depths of edge beams and for various width-to-span ratios. In the computations the width of the structure was kept constant (36 ft) whereas the length was varied. The effect of the edge displacements becomes more pronounced as the depth of the edge beam decreases, and as the width-to-length ratio decreases. In these computations the torsional resistance of the edge beam has been neglected as in Mr. Gaafar's analysis. For large edge beams this factor may be appreciable, particularly on the value of the transverse moments.

The variation of the ratio s_c/s_a for roofs with various numbers of plate elements with horizontal projections when acting with two stiff vertical edge beams of 7.5-ft depth is shown in Table 11. These values are for a constant width-to-length ratio of 0.288 and for a uniform vertical loading. In the range of cases investigated, the values indicate that the importance of edge displacements increased with the number of plate elements.

TABLE 11.—VALUE OF THE RATIO s_c/s_a FOR A WIDTH-TO-SPAN RATIO OF 0.288 AND AN EDGE-BEAM DEPTH OF 7.5 FT

Number of roof plates with horizontal projection	Top	Bottom
2	+0.041	−0.021
3	+0.034	−0.028
4	−1.64	+0.43
5	−2.39	+1.04

TABLE 12.—THE EFFECT OF EDGE-BEAM DEPTH ON THE STRESS AND TRANSVERSE MOMENT CORRECTIONS

Edge-beam depth, in feet	(a) $\frac{s_c}{s_a}$ – RATIO[a]		(b) $\frac{M'_c}{M_{ap}}$ – RATIO[b]		
	Three-segment roof	Five-segment roof	WIDTH-TO-LENGTH RATIO		
			0.288	0.407	0.576
7.5	+0.034	−2.40	0.26	0.07	0.02
3.75	+0.36	−2.40	1.58	0.52	0.12
1.875	+4.52	−2.74	4.11	2.11	0.72
0.9375	−3.42	−3.94	5.65	4.69	2.65

[a] At the top edge of an edge beam in a roof with a width-to-length ratio of 0.288. [b] At joint C in a three segment roof.

The importance of the number of plate elements extending over the width of the roof and of the stiffness of the vertical edge beams is further indicated by the results given in Table 12(*a*).

For a roof with five plate elements and two vertical edge beams, the results in Table 12(*a*) show that the approximate method is greatly in error even with extremely stiff edge beams. Evidently, the effect of the edge displacements on the longitudinal stresses can be several times the stress obtained from the approximate method which neglects the edge movement.

In Table 12(*b*) the effect of edge displacements on the transverse moments is shown for a three-segment roof with vertical edge beams subjected to uniform vertical loading. The ratio of M'_c (the correction of the moment at edge C

in the three-segment roof of Fig. 2) to M_{ap} (the same moment at edge C by the approximate method) is given for various depths of edge beams for various width-to-span ratios.

TABLE 13.—VALUE OF THE RATIO $\frac{M'_c}{M_{ap}}$ FOR FIVE-SEGMENT ROOFS

Edge-beam depth, in feet	Width-to-Span Ratio					
	0.288		0.407		0.576	
	Joint C	Joint D	Joint C	Joint D	Joint C	Joint D
7.5	−1.42	+1.20	−1.44	+1.07	−1.33	+0.96
3.75	+0.31	+4.51	−0.70	+2.08	−1.01	+1.13
1.875	+3.16	+10.22	+1.32	+5.39	+0.08	+2.04
0.9375	+4.91	+14.40	+3.88	+10.40	+2.38	+4.75

Table 13 gives results similar to those in Table 12(*b*) for a roof with five plate elements across the width and two vertical edge beams. Table 13 also illustrates the importance of the correction for edge displacement irrespective of the edge-beam depth or the width-to-span ratio.

A graphical illustration is shown in Fig. 30 of the effect of varying the stiffness of the edge beams and the width-to-span ratio on the value of the total transverse edge moment. The values, which are for a uniform vertical loading over the entire roof, have been determined by use of Mr. Gaafar's method of analysis.

A comparison is given in Fig. 31 of the actual longitudinal stress distribution at the midspan of a hipped plate structure of 36-ft width and spans of

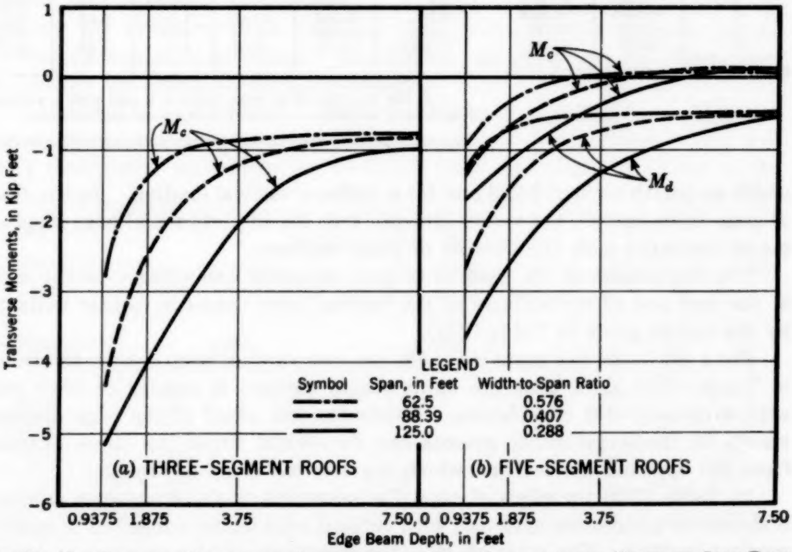

FIG. 30.—THE EFFECT OF VARYING THE STIFFNESS OF THE EDGE BEAMS AND THE WIDTH-TO-SPAN RATIO ON THE VALUE OF THE TOTAL TRANSVERSE MOMENT

62.5 ft, 88.39 ft, and 125 ft (as given by Mr. Gaafar's solution) to the corresponding values given by the ordinary beam formula assuming a linear distribution of stress. The ratio of the stress, s_g (that is given by the author's solution) to the corresponding value given by the ordinary beam formula, s_{ob}, is shown in Fig. 32 for the top and bottom edges for various width-to-span ratios and for various depths of edge beams. It is apparent that the assumption of a linear stress distribution is not sufficiently accurate for most structural arrangements.

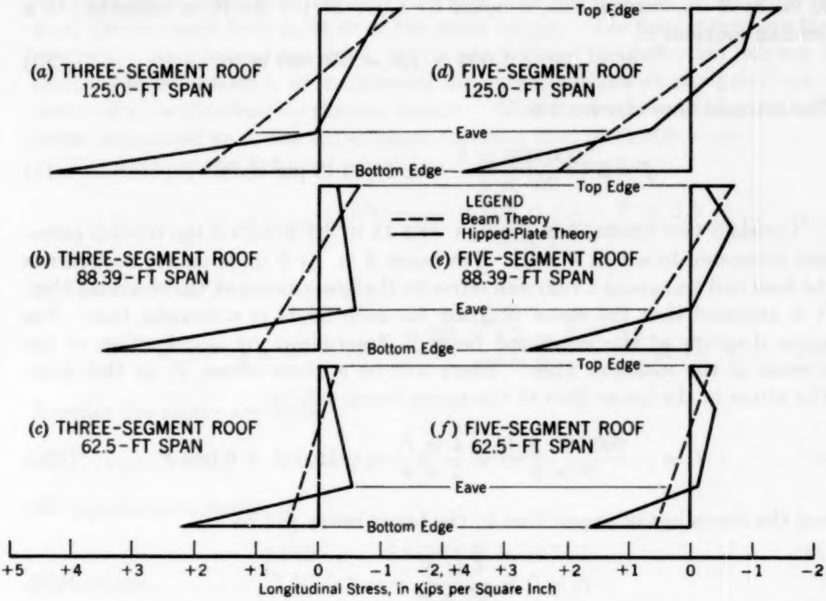

FIG. 31.—DISTRIBUTION OF THE LONGITUDINAL STRESS AT MIDSPAN (1.875-FT-DEEP EDGE BEAM)

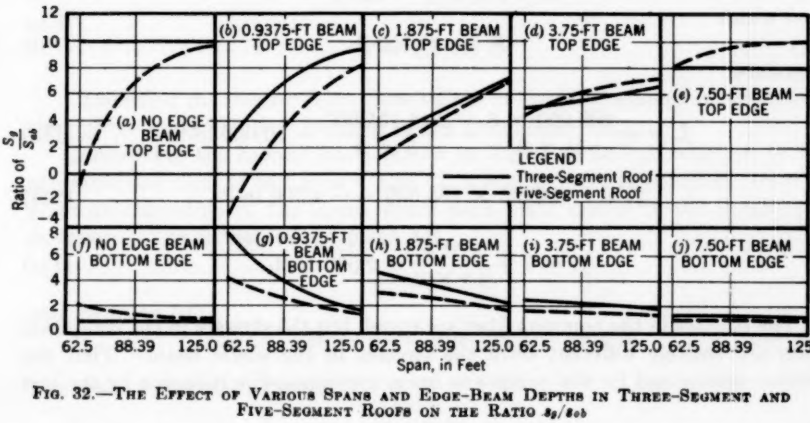

FIG. 32.—THE EFFECT OF VARIOUS SPANS AND EDGE-BEAM DEPTHS IN THREE-SEGMENT AND FIVE-SEGMENT ROOFS ON THE RATIO s_g/s_{ob}

R. Gartner,[16].—The value of Mr. Gaafar's paper is greatly increased by a

[16] Cons. Civ. Engr., Capetown, Union of South Africa.

model test. This makes it possible to compare actual stresses with stresses computed from various theories. The original theory, which the author terms the "approximate theory," is based on the equalization of stresses in the common fiber, and is quite inadequate. This inadequacy can be proved theoretically by the following example:

A 20-ft-long beam composed of monolithic material, with a cross section of 20 in. by 9 in., loaded with w equal to 1,000 lb per lin ft, is subjected to a bending moment of

$$M = 20^2 \times 1{,}000 \times 1.5 = 600{,}000 \text{ in-lb} \qquad (10)$$

The extreme fiber stresses are

$$f = \pm \frac{600{,}000 \times 6}{20^2 \times 9} = \pm\ 1{,}000 \text{ lb per sq in.} \qquad (11)$$

Consider two beams, 5 in. by 9 in. and 15 in. by 9 in., on top of each other, and connected to act as a unit. The beam 5 in. by 9 in. is on top and carries the load and transmits a common stress to the lower beam at the common fiber. It is assumed that the stress diagram for each beam is a straight line. The stress diagram of the combined beam is determined by equalization of the stresses of the common fiber. There will be a shear stress, F, in this fiber. The stress in the lower fiber of the upper beam will be

$$f_b = -\frac{600{,}000 \times 6}{5^2 \times 9} + \frac{4 \times F}{5 \times 9} = -\ 16{,}000 + 0.089\, F \qquad (12a)$$

and the stress in the upper fiber of the lower beam will be

$$f_b = 0 - \frac{4 \times F}{15 \times 9} = -\ 0.0296\, F \qquad (12b)$$

From Eqs. 12

$$-16{,}000 + 0.089\, F = -\ 0.0296\, F \qquad (13a)$$

from which

$$F = 135{,}000 \text{ lb} \qquad (13b)$$

Therefore,

$$f_a = + \frac{600{,}000 \times 6}{5^2 \times 9} - \frac{2 \times 135{,}000}{5 \times 9} = 10{,}000 \text{ in-lb} \qquad (14a)$$

$$f_b = -\ 0.0296 \times 135{,}000 = -\ 4{,}000 \text{ in-lb} \qquad (14b)$$

and

$$f_c = 0 + \frac{2 \times F}{15 \times 9} = 2{,}000 \text{ in-lb} \qquad (14c)$$

The stresses in the common fiber are equal, but the stresses in the composite beam are entirely different from the stresses in the single beam. That the stresses determined for the composite beam are impossible is shown by the fact

that, according to the stresses, the upper beam would be sagging, and the lower beam would be curved upward. Evidently, equalization of the common fiber stresses is inadequate, and a further condition must be imposed. It can be deduced that the upper beam presses down upon the lower, which therefore takes a part of the load, relieving the upper beam by the same amount, p. The distribution of p in the longitudinal direction is dependent on the deflection curve. As the beam deflects (as a result of a uniformly distributed load) p will also be uniformly distributed. Therefore, both deflection curves must have the same form, both should be sagging, and (on account of the equalization) the common fiber must have the same length. The two curves are then identical. As a second condition, either one point of the deflection line can be assumed to be common, or the slope of the deflection lines at any point can be assumed to be identical for the two beams. With the load carried by the lower beam designated as p, the upper beam carries a load of $(1,000 - p)$.

The angle of the deflected upper beam at the support is

$$E\gamma = \frac{1}{3} \times 20 \times 12 \, \frac{(1,000 - p) \times 20^2 \times 1.5 - F \times 2.5}{-5^3 \times 9} \times 12 \quad \text{(15a)}$$

and for the lower beam the angle is

$$E'\gamma = \frac{1}{3} \times 20 \times 12 \, \frac{p \times 20^2 \times 1.5 - F \times 7.5}{15^3 \times 9} \times 12 \quad \text{(15b)}$$

Because the angles are equal

$$280\,p + F = 270,000 \quad \text{(16a)}$$

the equalization results in

$$14.222\,p + 0.11874\,F = 16,000 \quad \text{(16b)}$$

from which

$$p = 844 \text{ lb} \quad \text{(17a)}$$

$$1,000 - p = 156 \text{ lb} \quad \text{(17b)}$$

and

$$F = 33,638 \text{ lb} \quad \text{(17c)}$$

Computing the stresses from these values in the same manner as previously, they prove to be identical to those of the monolithic beam.

Considering the hipped beam shown in Fig. 3 to be subjected to vertical experimental loads of 58.4 lb at C and C′, it is of interest to compute, from the given average stresses, the forces which each plate carries in the longitudinal direction. The forces are, for plate AB,

$$p_1 = 17.1 \text{ lb} \quad \text{(18a)}$$

and for plate BC,

$$W - p_2 = 108 - 38.5 = 69.5 \text{ lb} \quad \text{(18b)}$$

The shear forces are, at point B,

$$F_1 = 180.5 \text{ lb} \quad \text{(19a)}$$

and at point C,

$$F_2 = 163.3 \text{ lb} \quad \text{(19}b\text{)}$$

In contrast to Mr. Gaafar's solution, the load W is (in this case) the load at each third point of span L.

With these loads, the free moments are, for plate AB,

$$M_0 = \frac{35}{3} \times 17.1 = 199 \text{ in-lb} \quad \text{(20}a\text{)}$$

and for plate BC,

$$M_0 = \frac{35}{3} \times 69.5 = 810 \text{ in-lb} \quad \text{(20}b\text{)}$$

The final stresses are, at point A in plate AB,

$$f_{A,AB} = \frac{199}{0.1354} - \frac{2 \times 180.5}{0.325} = 1{,}470 - 1{,}110 = +\,360 \text{ lb per sq in.} \quad \text{(21}a\text{)}$$

at point B, in plate AB,

$$f_{B,AB} = -\,1{,}470 + 2{,}220 = +\,750 \text{ lb per sq in.} \quad \text{(21}b\text{)}$$

at point B, in plate BC,

$$f_{B,BC} = +\frac{810}{0.266} - \frac{4 \times 180.5}{0.455} - \frac{2 \times 163.3}{0.455}$$
$$= 3{,}050 - 1{,}590 - 718 = +\,742 \text{ lb per sq in.} \quad \text{(21}c\text{)}$$

at point C, in plate BC,

$$f_{C,BC} = -\,3{,}050 + 795 + 1{,}436 = -\,819 \text{ lb per sq in.} \quad \text{(21}d\text{)}$$

at point C, in plate CC′,

$$f_{C,CC'} = -\frac{2 \times 163.3}{0.455} = -\,718 \text{ lb per sq in.} \quad \text{(21}e\text{)}$$

The stresses computed in Eqs. 21 should be compared with those given in Col. 5, Table 6. The stress computed in Eq. 21e which should correspond to that of Eq. 21d has an error of 14%. If it is considered that the values of p_1, p_2, F_1, and F_2 vary slightly, this error is not too large—especially as the difference in stresses and deflections measured at the two sides of the model is, at some points, as great as 13%.

If the stresses computed by Mr. Gaafar are used rather than the stresses measured from the model, the following approximate values for the forces are obtained:

$$p_1 = 14.7 \text{ lb} \quad (22a)$$

$$W - p_2 = 108 - 25.8 = 82.2 \text{ lb} \quad (22b)$$

$$F_1 = 186 \text{ lb} \quad (22c)$$

$$F_2 = 210 \text{ lb} \quad (22d)$$

These values give very nearly the same stresses as those determined by Mr. Gaafar.

Conclusions.—It can be seen that mere equalization of stresses at the junction is not sufficient; another condition must be introduced in order to determine the actual stress conditions in a structure. The condition that Mr. Gaafar introduced seems to be adequate, but may be simplified if the exact equation can be used, together with the equation for equalization. Instead of using several steps, the solution could be obtained in one operation. More tests on larger models would be useful. In the model used by the author there seems to have been a slight twist, as the deflections on one side are all larger than the corresponding deflections on the opposite side. The method advanced by Mr. Gaafar is an important step forward in the solution of this problem.

IBRAHIM GAAFAR,[17] A. M. ASCE.—The interesting discussions contributed by Mr. Craemer, Messrs. Paulson and Maugh, and Mr. Gartner are gratifying to the writer.

[17] Asst. Prof. of Structural Eng., Ibrahim Univ., Cairo, Egypt.

The historical information to which Mr. Craemer has taken exception is true only of the work to which it referred—namely, Mr. Ehlers' work.[3] Mr. Craemer extended the statements about Mr. Ehlers' assumptions to his own works[5,6,8] which were referred to in another statement. That statement contained the facts restated by Mr. Craemer in his discussion—namely, that the current approximate theory, or "elementary theory," assumes the plates to be rigidly connected at the joints and takes into consideration the resulting transverse connecting moments but neglects the translation of the edges.

The sinusoidal treatment of edge translations has been questioned by Mr. Craemer on the basis that the transverse moments, claimed to be linearly related to them, would then be sinusoidal also, which is not true of systems in which the pure beam effect is approximated. However, the relation between transverse moments and edge displacements is not entirely linear. Transverse moments depend in part on the distribution of the external loads on the roof, and partly on the relative edge displacements (the word "relative" being particularly significant). They are therefore sinusoidal only in the latter part which has been thus computed, the former part having been computed through the approximate theory in the paper. Moreover, the more nearly a system approximates a beam, the smaller are the relative edge displacements; these relative displacements disappear entirely in the case of a pure beam system. Thus, in systems in which the pure beam effect is approximated, the sinusoidal part of the transverse moments nearly vanishes.

Can the proposed hipped plate theory be applied to a system having dimensions and load distribution such that the structure deforms like a beam? Will the proposed theory yield zero relative edge displacements and consequently indicate the longitudinal stresses computed by the pure beam theory or approximate theory? That this is so will be shown by applying the proposed theory to a pure beam system as follows:

Example No. 3.—The forces acting on a small element length dx of a beam loaded with a load w pounds per unit length, the beam cross section, and the shear stress diagram on that cross section are shown in Fig. 33. By equating to zero the moments about point u of all forces acting on prism 1 1 2 2, shown in Fig. 33(b), one may write

$$\int_m^n \frac{s_1 - s_2}{Y}\, y\, dA\, (y - D) - V'\, dx = 0 \quad \ldots\ldots\ldots\ldots (23)$$

in which V' is the vertical shearing force acting on the shaded area, A', of the cross section and y is the centroidal distance. Therefore, if prime superscripts designate properties of the shaded area in Fig. 33,

$$\frac{V'}{V} \doteq \frac{I' - A'\, y'\, D}{I} \quad \ldots\ldots\ldots\ldots (24)$$

The dimensions of the cross section of the aluminum model are given in Fig. 34.

$$I = 3.637 \text{ in.}^4 \quad \ldots\ldots\ldots\ldots (25a)$$

The moment of inertia of the sectional area of the plates AB and A′B′ about the neutral axis is

$$I' = 2.208 \text{ in.}^4 \quad \ldots\ldots\ldots\ldots (25b)$$

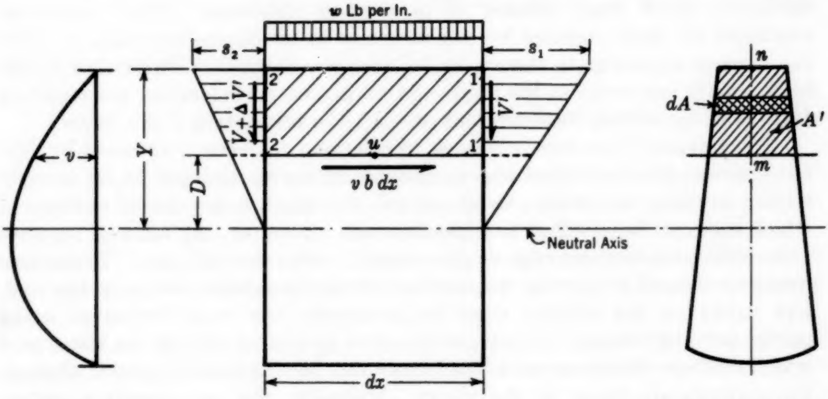

(a) SHEAR STRESSES (b) FORCES ON A BEAM ELEMENT (c) CROSS SECTION

FIG. 33.—STRESS DISTRIBUTION IN A BEAM

Thus, by Eq. 24, the portion V' carried by side plates AB and A'B' is 0.472 V lb. That is, under pure beam behavior, plates AB and A'B' carry 0.472 of the total load on the model.

The aluminum model will be analyzed for a uniform vertical line load of w lb per lin in. of the model, distributed along the edges in such a way as to produce pure beam deformation. The line-load distribution is shown in Fig. 35.

If the structure deforms as a beam, the analytical stresses at the midspan are

$$s_a = +w\frac{35^2}{8} \times \frac{2.945}{3.637} = +124\,w \quad \text{(26a)}$$

$$s_b = +18.7\,w \quad \text{(26b)}$$

and

$$s_c = -60.3\,w \quad \text{(26c)}$$

Analysis by Proposed Theory.—The P-forces, the free edge bending moments at midspan, and the free edge stresses for the different plates are computed in the same manner as in Example No. 1.

The free edge stresses are corrected to include the effect of edge shear forces by the procedure of Table 2. The stresses after correction are: At edge A, $+125.8\,w$; at edge B, $+16.4\,w$; and at edge C, $-59.75\,w$. These are nearly the same values as those of Eqs. 26.

In determining the effect of the relative displacements of the joints on stresses, all computations and results given in steps 2 and 3 of Example No. 1 are applicable. Hence, as in Eq. 6 and Fig. 14, $\delta_{ab} = -0.533 \times 10^{-3}\,w - 0.457\,\Delta$, and $\delta_{bc} = +0.265 \times 10^{-3}\,w - 0.2195\,\Delta$.

The same geometrical relation of Example No. 1 applies herein—namely, $\Delta = 1.186\,\delta_{ab} + 2.2071\,\delta_{bc}$. Substituting the values for δ_{ab} and δ_{bc} in this geometrical relation yields $2.026\,\Delta = (+0.585 - 0.633)\,10^{-3}\,w$, or $\Delta \approx 0.0$, the required condition for pure beam behavior. The values between the parentheses should have yielded zero; the discrepancy corresponding to an average of 2.5% change in approximate-theory stresses is caused by the small original difference between approximate-theory stresses and beam-theory stresses, and by slide-rule inaccuracies.

Example No. 4.—The aluminum model loaded with uniform line load $w/2$ lb per lin in. of edges C and C' (Fig. 36) has been analyzed by first assuming pure beam behavior as in Example No. 3 and then applying the two corrections

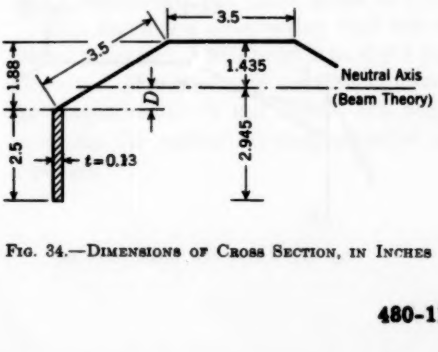

Fig. 34.—Dimensions of Cross Section, in Inches

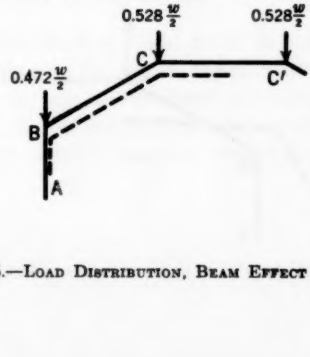

Fig. 35.—Load Distribution, Beam Effect

explained in the paper (under the heading, "Hipped Plates Compared with Ordinary Beams") and designated therein as corrections (*a*) and (*b*). Loads for correction (*a*) are shown in Fig. 37 and resemble those for correction (*b*) due to Δ, shown in Figs. 10 and 11(*a*). The stresses in terms of Δ due to the latter correction are the same as those due to Δ in any of the previous examples; and the stresses due to the former correction (*a*) are proportional to them. The procedure used in Example No. 1 in steps 4 and 5 serves to give the final results. The final stress values have been computed and appear in Table 14, Col. 5. The same problem has been analyzed by the proposed-theory procedure, and the results are given in Table 14, Col. 8.

TABLE 14.—MAXIMUM LONGITUDINAL STRESSES AT MIDSPAN

Edge	Example No. 4[a]								Example No. 2[e]		
	Beam-Theory Approach				Approximate-Theory Approach				Beam Theory	Corr'ns. (*a*) + (*b*)	Final Values
	Beam theory	Corrections		Final values	AT[b]	JD[c]	PT[d]				
		(*a*)	(*b*)								
(1)	(2)	(3)	(4)	(5)	(6)	(7)	(8)		(9)	(10)	(11)
C	− 60.3	− 92.2	+ 47.5	−105.0	−152.0	+ 47.5	−104.5		− 537	−383	− 920
B	+ 18.7	+205.3	−106.5	+117.5	+221.8	−106.5	+115.3		+ 166	+860	+1,026
A	+124.0	−236.0	+122.5	+ 10.5	−110.2	+122.5	+ 12.3		+1,102	−988	+ 114

[a] All values are to be multiplied by *w*, giving stresses, in pounds per square inch. [b] Values computed by the approximate theory. [c] Values resulting from relative displacements of joints. [d] Values computed by the proposed theory. [e] Stresses, in pounds per square inch.

Example No. 2 has been analyzed from the beam action approach, and the results are given in Table 14 for comparison with those of Table 6. Although both approaches (Table 14) lead to practically the same results, the proposed-theory approach, being the shorter, is the better.

Any single-span, symmetrically loaded hipped plate system can be solved by the technique of the proposed theory either by beginning from the pure shell effect (as in the writer's paper) or from the pure beam effect, and correcting for external load distribution and edge translations.

These examples answer Mr. Craemer's question as to the range of applicability of the analytical treatment developed in the paper. They show it to be generally applicable within the working conditions defined. Although ap-

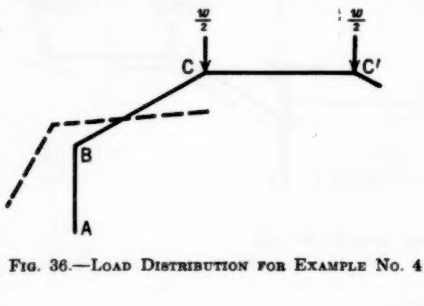

FIG. 36.—LOAD DISTRIBUTION FOR EXAMPLE NO. 4

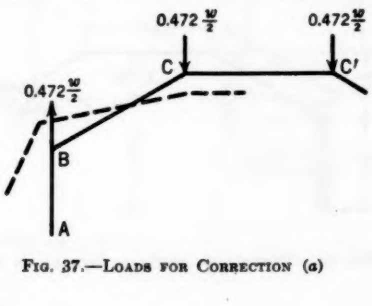

FIG. 37.—LOADS FOR CORRECTION (*a*)

plication of the method is generally possible, it is not always advisable. To correct for relative edge displacements where they are too small will not be worth while, and the approximate theory will be accurate enough. Mr. Craemer's investigation[13] serves to indicate qualitatively where the proposed theory might profitably be applied, as is also indicated by Messrs. Paulson and Maugh in their valuable discussion. However, the writer does not consider Mr. Craemer's method a safe indicator for systems that approximate a beam since a beam system will become a hipped plate system through a slight change in the distribution of loads. In Example No. 3, for instance, if the loads on the joints are made 0.5 $w/2$ each, instead of 0.472 $w/2$ and 0.528 $w/2$, the plates will rotate slightly, and the system will become a hipped plate system although ω—the practical indicator—remains unchanged ($\omega = L/H \sqrt{t/h}$). The system of Example No. 3 has been changed to a hipped plate system in Example No. 4 by changing the distribution of loads. This shows clearly that a pure beam system is a special case of a hipped plate system, not a limiting case as indicated by Mr. Craemer.[18]

[18] "Design of Prismatic Shells," by H. Craemer, *Journal*, A.C.I., No. 6, February, 1953, p. 558, Fig. 11.

It is interesting to compare the conclusions Messrs. Paulson and Maugh deduced from examples they solved using the proposed theory with similar conclusions deducible from the paper by Mr. Craemer.[13] Studying Fig. 11 for open sections in Mr. Craemer's paper,[18] the deviation of the longitudinal stresses (when edge translations are considered) from those due to the approximate or pure shell theory ($\omega = 0$) is seen to increase as ω increases. This result agrees with the conclusions reached by Messrs. Paulson and Maugh using the proposed theory—namely, s_c/s_a increases as L increases, as the depth of the end beams decreases, and as the number of plates increases—that is, as h decreases. The writer is especially interested in the agreement between results obtained by the two entirely different methods of treatment of Mr. Craemer and the writer.

Mr. Gartner has used the average longitudinal stresses measured at the edges of the model (Fig. 27) to compute the forces resisted by each plate in the longitudinal direction and shows his results in Eqs. 18 and 19. These forces are used to compute the stresses in Eq. 21. However, in this computation, Mr. Gartner has overlooked the fact that the average measured longitudinal stresses as shown in Fig. 27 are not exactly linear across each plate. The corresponding strains appear in Fig. 23(a). This oversight explains the discrepancies in the values of stresses obtained in Eq. 21. The slight curvature was considered in the check given in Table 9.

Mr. Gartner's observation that the deflections show a slight twist in the model is correct. The twist is so slight that its effect on the results is negligible. However, Mr. Gartner's suggestion concerning the use of the exact equation for simplification is not clear. His suggestion of eliminating the steps and reducing the method to one operation is, in the writer's opinion, out of the question.

DISCUSSION OF LIVE LOADING FOR LONG-SPAN HIGHWAY BRIDGES
PROCEEDINGS-SEPARATE NO. 198

LOUIS BALOG.[8]—Specifications for the design live load of long-span highway

[8] Cons. Engr., Binghamton, N. Y.

bridges are incomplete without simultaneous reference to the permissible structural deformations. When the recommended live loads (listed in Table 4 and shown in Fig. 4) for computing deflections in accordance with the AASHO specifications (12)[8a] are used, bridges result that have an excessive

[8a] Numerals in parentheses, thus (12), refer to corresponding items in the Bibliography at the end of this discussion.

vertical rigidity. The importance of the consideration of the actual deflection is indicated by the proportions and behavior of the bridges listed in Table 6. Schematic cross sections of these bridges are shown in Fig. 5.

The slender girder bridges built in Germany and listed in Table 6 could not have been built if their design live loads (which also included railway loadings) had been used in computing the permissible deflections in conformity with the AASHO specifications. It is always possible to satisfy the requirements pertaining to reasonably allowable stresses for the design live load if proper specifications permit deformations consistent with the safe use of the bridge.

Vertical Deflections.—The relation between the deflections caused by the design live load and the deflections caused by the actual live load is indicated by the results of the measurements made on the Köln-Deutz Bridge during the period from January, 1949, to March, 1949 (13). The movements of targets attached to the bridge at sections A and B were observed with a theodolite located as shown in Fig. 6(*a*). Figs. 6(*c*), 6(*d*), and 6(*e*) show the measured maximum vertical deflections (increased by vibrations) caused by peak traffic containing moving load concentrations (of weight and length shown) at recorded locations. The bridge was not noticed to have moved laterally. The smallness of the largest values of the measured deflections furnishes a scale for the improbability of the occurrence of design live-load deflections.

TABLE 6.—CONTINUOUS PLATE GIRDER BRIDGES WITH MONOLITHIC STEEL FLOORS

Bridge Location (Germany)	Year completed	Length of girder, in feet[a]	LENGTH OF SPANS, IN FEET				SPAN-TO-DEPTH RATIO[b] FOR LONGEST SPAN	
			Span 1	Span 2	Span 3	Span 4	Midspan	Support
Köln-Deutz	1948	1434.75[c]	433.51	605.15	396.09		57.9	24.0
Bonn-Beuel	1949	1292.64[c]	324.80	643.04	324.80		65.0	24.0
Kurpfalz, Mannheim	1950	613.52[c]	184.05	245.40	184.05		54.8	23.7
Düsseldorf-Neuss	1951	1351.70[d]	337.925	675.85	337.925		61.9	26.3
Smidt, Bremen	1952	724.40[d]	207.5	100.2	100.2	49.2	41.7	41.7

[a] Center to center of end bearings for the main river unit. [b] Average outside depth of steel. [c] Riveted construction. [d] Welded construction, riveted field connections.

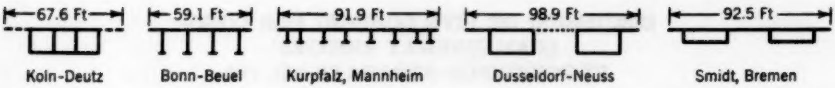

Fig. 5.—Schematic Cross Sections of the Bridge Listed in Table 6

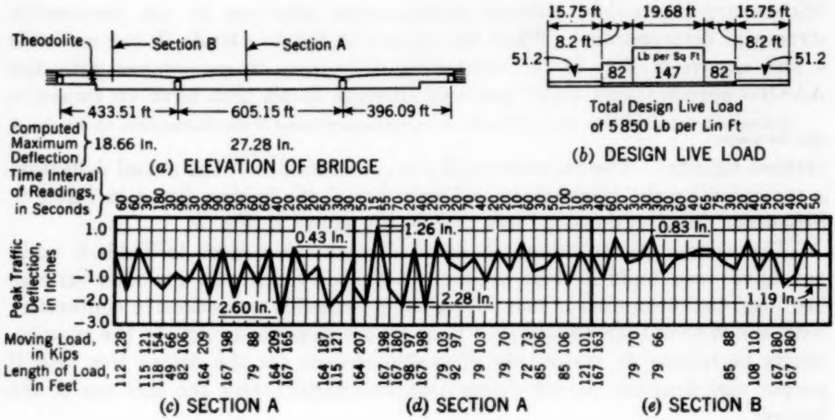

Fig. 6.—Design Live Load, Measured Peak Loadings, and Maximum Deflections of Bridge at Köln-Deutz (Germany)

The measured maximum deflections at sections A and B were 1/2,790 and 1/4,360 of the span. In contrast, maximum deflections of 1/266 and 1/279 of these spans were computed for the design live load (14). The computed design live-load deflection of the Düsseldorf-Neuss Bridge is 1/230 of the center span (15) and those of the Kurpfalz Bridge are 1/359 and 1/488 of the center and side spans, respectively. The AASHO specifications (12) limit the deflection caused by the design live load plus impact to 1/800 of the span, and thus rule out the aforementioned bridges which are sufficiently rigid. These bridges are also eliminated by the requirements for the span-to-depth ratios of girders.

The accuracy of evaluating the magnitude and location of the traffic loads on the Köln-Deutz Bridge received consideration. The deflections computed for the traffic loads (without knowledge of the measured values) were in satisfactory agreement with the measured values when a composite moment of inertia was used in the compressed lengths of the concrete flooring. When only the moment of inertia of the steel sections was used, the computed values increased 15% at Section A and 6.5% at Section B (13). Three significant facts have to be considered relative to the deflections of this structure: (*a*) The

design live-load deflection is three times larger than that permitted by the AASHO specifications (12). (*b*) The actual maximum measured deflection was less than 10% of that caused by the design live load. (*c*) The bridge is so stiff torsionally that its tilting is negligible.

Torsional Deflections.—The design live load located at the half width and full length of the center span produces 0.13% maximum transverse tilting of the Köln-Deutz Bridge. With a similar load at the center span and at the opposite half width of the side spans of the Düsseldorf-Neuss Bridge, the maximum tilting is 0.4% (15). Test loading with vehicles weighing 1,450 lb per lin ft placed along the curb in two thirds of the center span of the Kurpfalz Bridge produced a maximum tilting of 0.21%. The moment caused by this loading was slightly greater than 20% of the maximum torsional moment produced by the design live load.

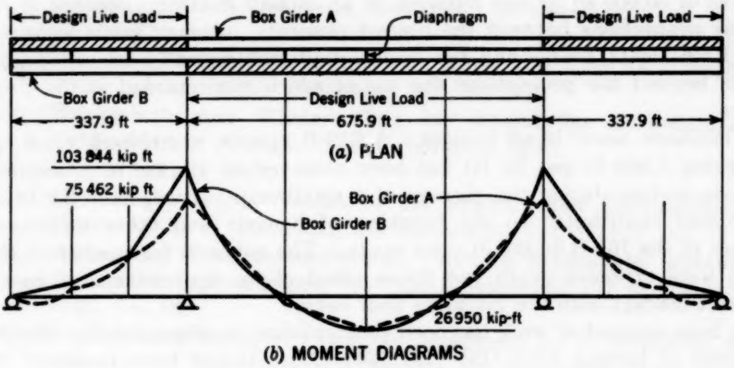

FIG. 7.—EFFECT OF DIAPHRAGMS IN EQUALIZING TORSIONAL LOADING OF BRIDGE AT DÜSSELDORF (GERMANY)

Fig. 7 shows the loading producing the maximum computed transverse tilting of the Düsseldorf-Neuss Bridge and the corresponding moments (15). It appears that diaphragms 20 ft long, two in the side spans and three in the center span, greatly equalize the moments between the two box girders. In the Smidt Bridge, cross frames, 23 ft long, spaced 68.9 ft and 78.7 ft in spans of 367.5 ft and 207.5 ft, respectively, assure that the four webs of the two box sections, about 23 ft wide and 8 ft deep, carry approximately equal shares of the torsional loadings of the bridge. The torsional deformations of these slender bridges are small.

Vibrations.—The vibrations of the spans of the Köln-Deutz Bridge resulting from rail traffic could be detected only by instruments. Occasionally, light trucks caused noticeable, slight vibrations of the longer side span. Vibrations of small amplitudes and frequencies of from 20 cycles per sec to 30 cycles per

sec were observed at the handrails located at the ends of the 15-ft-long brackets. The computed natural frequency of the bridge is 0.4 cycles per sec and, with the design live load placed over the entire bridge, the fundamental frequency is 0.3 cycle per sec (14).

German highway-bridge specifications (16) limited deflections to 1/500 of the span and permitted larger deflections for long spans without defining the limits of the deflections. Giving primary consideration to the fact that the slow vibrations of bridges were unnoticeable, Fritz Leonhardt made reference to the low natural frequency of the bridge and suggested that the permissible relative deflections of long-span bridges of low natural frequency be larger than for shorter spans of higher natural frequency (14). The behavior of the Köln-Deutz Bridge justified the basic characteristics of the design.

The experiences gained in the construction of the Köln-Deutz Bridge were utilized in the design of bridges built subsequently. The 4.72-in. concrete flooring (with exposed riding surface, anchored to steel-plate flanges having an area of 50,000 sq ft) was replaced by an asphalt flooring. Instead of rigid mortar connections between the precast elements, bitumen joints were used. The Köln-Deutz Bridge and the bridges built subsequently advanced girder design beyond the proportions the use of which was retarded in the United States.

Vibrations occur in all bridges. A 250-ft simple, camel-back truss span (weighing 7,000 lb per lin ft) has been observed to vibrate in a noticeable no-node motion during the passage of a small empty truck over the bridge. Vibrations contributed to the breaking of hangers and other members of bridges in the 100-ft to 600-ft span range. The common features of all these spans were excessive depth and frame effect of the broken vertical member in direct contact with the vibrating floor beam.

A large amount of work has been accomplished in measuring the vibratory behavior of bridges (17) (18) (19) (20) (21). It has been predicted that developments in highway traffic will necessitate improvement of the dynamic characteristics of vehicles and structures. The actual effect of the vehicle on the structure is not expressed by the weight and the impact factor. The response of the bridge to these effects, however, depends on structural proportions and arrangements influencing dynamic behavior.

Conclusions.—The probability of the occurrence of the design live load decreases with increasing span and varies with bridge locations. Deflections and vibrations caused by the actual traffic govern the satisfactory behavior of long-span bridges not subject to objectionable wind vibrations.

Traffic-load observations and deflection and vibration measurements should be simultaneous in order to avoid the formulation of inconsistent specifications that arbitrarily limit the structural proportions and deflections.

The refinements in "balanced design" involve unattainable accuracy in making, shaping, fabricating, assembling, and erecting structural steel. These refinements are also unsuited for defining the factor of safety of various structural arrangements. Assuming standard quality materials, workmanship, and reasonable details, the magnitude of the stresses depends on the distribution of the actual loads, and the amplification of the stresses depends on the vi-

bratory characteristics of the loads and of the structural arrangements. The specification of allowable-stress computations which only complicates the design should be avoided.

Specifications that do not agree with the actual behavior of structures hinder the use of existing knowledge. They present an obstacle to the use of available materials and to the development of efficient structural arrangements. The infrequent issuance of specifications and the rapid advances in structural techniques demand that any specification which is issued contain specific statements concerning its limited validity.

Bibliography.—

(12) **"Standard Specifications for Highway Bridges,"** Am. Assn. of State Highway Officials, Washington, D. C., 5th Ed., 1949.

(13) **"Beitrag zur Frage der Durchbiegung von grossen Strassenbrücken im Zusammenhang mit Messungen an der Köln-Deutzer Rheinbrücke,"** by Franz Braun and Fritz Barth, *Der Bauingenieur*, Vol. 26, 1951, pp. 65–67.

(14) **"Die neue Strassenbrücke über den Rhein von Köln nach Deutz,"** by Fritz Leonhardt, *Die Bautechnik*, Vol. 26, 1949.

(15) **"Denkschrift zum Wiederaufbau der Rheinbrüke Düsseldorf-Neuss 1950–1951,"** J. Springer, Berlin, Germany, 1951.

(16) **DIN 1072, April, 1941.**

(17) **"Grundzüge für ein Verfahren zur dynamischen Untersuchung von Brücken,"** by N. Streletzki, *Die Bautechnik*, Vol. 5, 1927, No. 41.

(18) **"Beitrag zur Brückenmesstechnik. Neuere Messungen dynamischer Brückenbeanspruchungen,"** by Rudolf Bernhard, *Der Stahlbau*, Vol. 1, 1928, No. 13.

(19) **"Stosswirkung bewegter Lasten auf Brücken,"** by N. Streletzki, *Bericht uber die II*, Internationale Tagung für Brückenbau und Hochbau, Wien, 1928, J. Springer, Vienna, Austria, 1929.

(20) **"Brücke und Fahrzeug, Betrachtungen über ihre dynamischen Zusammenhange,"** by Rudolf Bernhard, *Der Bauingenieur*, Vol. 11, 1930, No. 28.

(21) **"Dynamische Untersuchungen von Brücken und Hochbauten,"** by G. Reutlinger, *Publications*, IABSE, Leemann, Zurich, Switzerland, Vol. 1, 1932, pp. 387–410.

Glenn B. Woodruff,[9] M. ASCE.—The writer appreciates the immense

[9] Cons. Engr., San Francisco, Calif.

amount of work performed by the authors and joins in the hope that there will result a standardization of specifications for long-span highway bridges. It is also hoped that further work may develop data that will lead to the improvement of specifications for bridges of shorter span. Although the chief purpose of the authors has been the proposal of a loading for long-span bridges, consideration has been given to related subjects.

Certain data and conclusions obtained by the authors can be summarized as follows:

1. The AASHO H20-S16-44 loading is accepted for spans of less than 600 ft. Assuming an increase of $\frac{1}{3}$ in this loading, an allowable base stress of 24 kips

per sq in. for carbon steel is proposed.

2. The greatest loads (where more than one vehicle is involved) occur when traffic is stalled. Under this condition there are no dynamic forces.

3. On traffic lanes restricted entirely to commercial traffic, the percentage of the heavier vehicles is very small.

It can also be stated that:

a. It is the concensus of highway engineers that it is not economical to design pavements for loads exceeding legal limits. Unfortunately there will always be some cases of illegal loads exceeding such limits.

b. There exists little definite knowledge as to the magnitude of dynamic stresses in highway bridges. Such data as is available indicate that the AASHO specifications are conservative in this respect.

c. The history of both highway and railway bridges has been that of over-designed trusses and girders in comparison with the design of the floor system.

The writer endorses the opinion of the authors that the design should be based on the largest combination of stresses that are probable during the life of the structure and should use the greatest unit stresses that are prudent. The authors mention various methods of achieving the result, but fail to mention the method which assumes the greatest probable live load and combines the stresses therefrom with those produced by other forces. Moreover, there appears little logic in restricting this proposal to "large structures." If a given unit stress is satisfactory in the chord of a long-span bridge, it should be even more conservative in the flanges of a plate girder or rolled beam.

The safety factors listed in Table 5 may be misleading because no provision is made for increase of live load. If the live load were increased by $\frac{1}{3}$, the factor would become 1.5 throughout. In addition to stresses produced by dead, live, and dynamic loadings, other stresses result from lateral and longitudinal forces and from changes in temperature. The stresses are not uniformly distributed across the member (22)[9d](23).

[9d] Numerals in parentheses, thus: (22) refer to corresponding items in the Bibliography at the end of this discussion.

The safety factors also may be misleading because the upper yield point, as determined by the mill "drop of beam" test, is above the true elastic limit.

It is wasteful to use a stress of 18 kips per sq in. for A-7 steel, but an increase of $\frac{1}{3}$ is not recommended unless an allowance is included for the effects previously listed.

There are considerable data enabling the engineer to evaluate the heaviest probable single vehicle. From this point, the matter becomes one of selecting the most severe probable combination of these loads in a single lane, and then of combinations of these heavy loads in additional lanes. For a single lane, it appears logical to assume a vehicle (type S-2) loaded to the legal limit, and to add $\frac{1}{3}$ to allow for illegal loading and other "unmeasurables." To this loading, it would be necessary to add an allowance for impact. For longer spans, an unusual (but possible) situation would be for any combination of three vehicles, one as previously described, the other two of the same type but loaded to legal limit, to "close up." In this case, no impact would be involved.

Assuming that the ultimate or maximum live loads are being considered, the H20-S16-44 loading—as well as those loadings recommended by the authors—appears to be inadequate. However, the probabilities of simultaneous loading in the other lanes are such as to justify a greater reduction than that permitted by the AASHO specifications. Accordingly, the writer proposes the following loadings:

1. Single Lane.—A vehicle (type 3-S2) with axle loads of 12 kips, 24 kips, 24 kips, 24 kips, and 24 kips, and axle spacing of 16 ft, 4 ft, 16 ft, to 30 ft, and 4 ft. To this loading, impact should be added according to the AASHO formula. This loading may be replaced by a uniform load of 800 lb per lin ft for spans of less than 1,100 ft and 720 lb per lin ft for longer spans with moment concentrations of 60 kips for spans of less than 600 ft, 300 kips for spans of between 600 to 1,000 ft, and zero kips for spans greater than 1,000 ft and shear concentrations of 80 kips for spans of less than 600 ft, 40 kips for spans of between 600 ft to 1,000 ft, and zero kips for spans greater than 1,000 ft. No impact should be added to these loads.

2. Additional Lanes.—One hundred percent of the load listed for a single lane is assumed in the lane nearest the truss being considered, 75% of the single-lane load in the lane farthest away from the truss being considered, and 25% of such load for a single lane in the other lanes.

A comparison of this proposal with that of the authors is shown in Table 7.

TABLE 7.—Comparison of Stresses Obtained by use of the Authors' Loading and the Proposed Loading

Span, in feet	Number of lanes	Distance between curbs, in feet	Center-to-center distance for trusses, in feet	Live Load Plus Impact Stresses per Truss			
				Proposed Loading		Authors' Loading[a]	
				Maximum moment, in kip-feet	Reaction, in kips	Maximum moment, in kip-feet	Reaction, in kips
300	2	26	31	14,500	220	11,100	158
300	4	52	57	16,800	256	16,400	232
600	2	26	32	43,300	300	35,000	238
600	4	52	58	50,500	349	53,300	363
1,000	4	52	58	125,000	500	139,000	554
1,000	6	76	82	150,700	603	181,000	720
1,500	4	52	58	253,000	674	288,000	768
1,500	6	76	82	305,000	814	375,000	1,000

[a] Assuming reduction for multiple lanes in accordance with AASHO specifications. For four-lane bridges maximum stress occurs with three lanes loaded.

The authors' proposal (for ultimate loads) appears to be low for two-lane bridges and excessive for bridges of four and six lanes.

A satisfactory live load is only part of a needed specification for the design of long-span highway bridges. The writer hopes the authors will continue their work in such a direction.

Bibliography.—

(22) **"Investigation of the Dead Load Stresses in the Mississippi River Veterans Memorial Bridge at East St. Louis, Illinois,"** by L. T. Wyly, R. W. Kluge, K. H. Lenzen, L. B. McGammon, M. B. Lagaard, and E. W. Larson, Jr., *Proceedings-Separate No. 219,* ASCE, July 1953.

(23) **"Investigation of the Dead Load Stresses and Live Load Stresses in a 350 Ft Truss Span on the A.T. and S.F. System,"** *Committee 30 Bulletin 509,* A.R.E.A., June–July, 1953.

WILLIAM G. BYERS,[10] J.M. ASCE.—The value of the author's paper is largely dependent on the value of the live loadings recommended in Table 4. These live loadings can best be evaluated by devising a standard of requirements for design loads in general and comparing the proposed loadings with the standard loadings.

[10] Draftsman, Gulf, Colorado, and Santa Fe Ry. Co., Galveston, Tex.

It is suggested that the following requirements be used for the design loads: (*a*) The design load should produce stresses approximately equal to those caused by the maximum load that is likely to be carried by the structure. This maximum load should be estimated on the basis of the loads currently being carried by comparable structures with an allowance for probable future increases. (*b*) The design load should give only one value of live load for a given span length or loaded area. (*c*) The load pattern should be simple. (*d*) The design load should reflect actual conditions whereby the total live load never decreases with an increase in the span length.

The author's proposed loading will satisfy the first three requirements if the larger of the two given values is specified for span lengths at which the load changes. The loading satisfies the fourth requirement except for span lengths near those at which the load changes. For example, the total load decreases 40,000 lb per lane as the span increases beyond 1,000 ft, and an additional inincrease of 66.7 ft is required to allow for the loss in total load. This condition could be remedied by using the following:

For spans of less than 500 ft, an H-20-S-16-44 loading should be used. This loading is represented by (1) w equal to 640 lb per ft, (2) the concentrated load for moment P_m equal to 18,000 lb, and (3) the concentrated load for shear P_v equal to 26,000 lb.

For spans of from 500 ft to 900 ft, w should equal 640 lb per ft; P_m should equal $18{,}000 - 45(L - 500) = 40{,}500 - 45\,L$; and P_v should be made equal to $26{,}000 - 65(L - 500) = 48{,}500 - 65\,L$.

For spans of from 900 ft to 1,300 ft, w should equal $640 - 0.2\,(L - 900) = 820 - 0.2\,L$, and P_m and P_v should both equal zero.

For spans that exceed 1,300 ft, w should equal 560 lb per ft, and P_m and P_v should both equal zero.

These recommendations are no more complex than the AASHO impact formula and could be combined with it, if desired, to give values of live load plus impact.

KUANG-HAN CHU,[11] A.M. ASCE.—There is no doubt that the loading

[11] Structural Designer, D. B. Steinman, Cons. Engr., New York, N. Y.

specified in the existing (1953) AASHO specification is too high for long-span bridges, although there is some question as to the intensity that should be specified. The step loading suggested by the authors has some disadvantages. At the point where the loading changes from one step to another, the sudden changes in stress (although small in comparison to the total dead-load and live-load stress—but not small in comparison to the live-load stress) are nevertheless inconsistent. The percentage change of stress when the influence lines are similar to those shown in Figs. 8(*a*) and 8(*b*) (as in continuous bridges or arch bridges) may exceed those predicated by the authors (8% of live-load stress or 2% of total dead-load and live-load stress). Moreover, when the influence line is similar to that shown in Figs. 8(*a*) and 8(*b*), the higher intensity of loading for one step with shorter loaded length (L_1) may produce much greater stress than the loading in the next step with a loaded length between the zero points of the influence line (L_2). A loading which varies continuously with loaded length is preferable to step loading. In Table 8 are included suggested

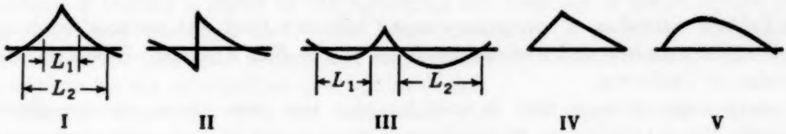

FIG. 8.—TYPES OF INFLUENCE LINES

TABLE 8.—LOADING SYSTEMS

LOADED LENGTH l, IN FEET	LOADING TYPE	EQUATION FOR ω	CONCENTRATED LANE LOAD, IN POUNDS	REMARKS
400 to 800	A, for moment	$\omega = 400 + \frac{480{,}000}{l + 1{,}600}$	18,000	For negative moment of continuous spans (in Fig. 7(c) $l = L_1 + L_2$), two concentrations, each at a different span, shall be used.
	B, for shear	$\omega = 440 + \frac{200{,}000}{l + 600}$	26,000	...
Greater than 800[a]	C, for shear and moment	$\omega = 430 + \frac{330{,}000}{l + 700}$	...	For negative moment of continuous spans (in Fig. 7(c) $l = L_1 + L_2$), one concentration of 18,000 lb, placed so as to produce the maximum stress, shall be used.

[a] The loadings A and B (used for spans of from 400 ft to 800 ft) can also be used for spans that are greater than 800 ft, but loading C is simpler and therefore recommended.

systems of loading which correspond closely with the authors' loading system and the data presented. In Table 8, ω is the uniform lane load in pounds per foot per lane.

The values given in Table 9 were obtained by using the loadings specified

TABLE—9. EQUIVALENT UNIFORM LOAD, IN POUNDS PER FOOT PER LANE

Loaded length, in feet	AUTHORS' LOADING		SAN FRANCISCO-OAKLAND BAY BRIDGE		LOADING TYPE		
	Moment	Shear	Maximum	Average	A	B	C
400	730	770	760	725	730[a]	770[a]	730
600	700	727	695	660	678[a]	694[a]	684
	670	683					
800	663	673	647	610	645[b]	648[b]	650[a]
	640	640					
1,000	640		610	575	620[b]	617[b]	624[a]
	600						
1,200	600		600	560	601[b]	594[b]	604[a]
	560						
1,500	560		600	550	579[b]	570[b]	580[a]
2,000	560		...	...	551[b]	543[b]	552[a]
3,000	560		...	...	516[b]	513[b]	519[a]
4,000	560		...	...	495[b]	497[b]	500[a]

[a] Recommended values. [b] Alternative values.

in Table 8 (based on a triangular-shaped influence line), the authors' loading, and the maximum and average loadings of the San Francisco-Oakland Bay Bridge in California.

Any concentration that is considerabley less than those concentrations specified by AASHO loses its significance in representing high concentration of axial load. Moving concentrations are useful in accounting for the effect of local load concentration in continuous bridges or arch bridges with influence lines similar to those shown in Figs. 8(*a*) and 8(*b*). The effect of the loads diminishes with increase in loaded length. With influence lines of the type shown in Fig. 8(*b*), loading B (with its high concentration) will produce approximately the same stress as loading A or loading C for l greater than 1000 ft. However, with influence lines of triangular shape (Fig. 8(*d*)), loading B is slightly less than loading A or loading C for l in that range (Table 9). With influence lines of the types shown in Figs. 8(*d*) and 8(*e*), the uniform loads of loading C will always give stresses equal to or higher than those given by loading A or loading B (for l greater than 800 ft). From the comparison shown in Table 9, it appears that, if continuous-loading curves should be adopted in some set of specifications, some loading system similar to that suggested by the writer may merit consideration.

R. J. IVY,[12] A. M. ASCE, T. Y. LIN,[13] M. ASCE, STEWART MITCHELL,[14] M. ASCE, N. C. RAAB,[15] M. ASCE, V. J. RICHEY,[16] A. M. ASCE, AND C. F. SCHEFFEY,[17] J. M. ASCE.—The Joint Committee wishes to thank those who discussed the paper. The interest shown, and the variations in the proposed loadings, emphasize the need for a standardized live loading for highway

[12] Superv. Bridge Engr., State Div. of Highways, Sacramento, Calif.

[13] Associate Prof. of Civ. Eng., Univ. of California, Berkeley, Calif.

[14] Prin. Bridge Engr., State Div. of Highways, Sacramento, Calif.

[15] Projects Engr., San Francisco Bay Toll Crossing, Berkeley, Calif.

[16] Sen. Bridge Engr., San Francisco Bay Toll Crossing, Berkeley, Calif.

[17] Asst. Prof. of Civ. Eng., Univ. of California, Berkeley, Calif.

bridges; the various opinions expressed in these discussions will be of great value to any group writing such a specification.

The writers restate their premise that the basis of a standardized live loading for long-span bridges should be the actual vehicles and traffic patterns found on the highways. It is believed that a "hand-picked" loading would be viewed with skepticism by the users of any such loads.

It is also recommended that the loading be presented in a form easy to use and familiar to most designers. Equations, curves, or tables should not be required in order to determine the proper load for each different loaded length. The writers are of the opinion that the steps in their proposed loading result in an ease of application that outweighs the hypothetical inaccuracy resulting therefrom.

Mr. Woodruff believes that the safety factors listed in the paper (Table 5) may be misleading. These factors were given as an example to illustrate the problem rather than as a definite conclusion.

Any increase in live loading during a period of several years affects all highway structures, and probably the only practical way of providing for a large increase in loading is either by strengthening the members of the structure or by decreasing the dead load. The latter procedure is probably the most practicable for long-span bridges and in most cases is accomplished in highway structures by the substitution of a lighter deck.

Messrs. Byers and Chu are concerned with the steps in the writers' proposed loading; both present alternate loadings in the form of equations which result in a lane loading that varies inversely with the loaded length. The writers considered such loadings and rejected them because of the complexity of application and loss of identity with the present AASHO standard live loads (12).

It should be noticed that the steps in the writers' loading curves occur in loaded lengths of more than 600 ft, on which the live loads, when used with other loading combinations, are a small percentage of the total design load used in the proportioning of structural members. This loading was recently applied to a large structure, now (1954) in the course of construction, with no recalculation of stresses and with ease of application.

The results in Table 9, based on live-load stresses, illustrate the close relationship of the loadings with those actually used and suggested. The writers remain convinced that not less than the 560-lb lane load should be used for spans exceeding 1,200 ft as most structures in this range (site conditions permitting) are suspension bridges, for which dead loads are not considered in the proportioning of the stiffening truss members.

As stated in the original paper, many related subjects must be considered before a comprehensive specification for long-span highway bridges can be formulated. As suggested by Mr. Balog, each subject, such as deflection, vibration, impact, and fatigue, merits a separate detailed study. The authors did not presume that their paper covered all phases of long-span bridge design. However, they believe that the adoption of a reasonable live loading for long-span bridges will lend impetus to the study of other conditions affecting structures.

DISCUSSION OF WIND LOADS ON TRUSS BRIDGES
PROCEEDINGS-SEPARATE NO. 201

J. M. BIGGS,* A.M. ASCE.–Prof. Farquharson has raised a very pertinent question regarding the validity of small scale wind tunnel tests when applied to wind loads on actual structures.

The tests described in the paper were conducted at Reynolds' Numbers ranging from 18,000 to 70,000 using the average width of the truss members normal to the wind direction as the representative dimension. No variation of drag coefficient within this range was detected. A 100 MPH wind on the prototype would correspond to a Reynolds' Number of 2,800,000. The results presented are of course applicable only if the drag coefficient is constant within the range of R which includes both model and prototype.

Theory indicates that for sharp-edged elements such as flat plates or structural members one should expect a constant C_D throughout this entire range of R. Prof. Farquharson states that test data to verify this conclusion for flat plates are very meager. This is true of rectangular plates but considerable information is available for sharp-edged circular disks. These data verify the theoretical conclusion since the drag coefficient was found to be constant for values of R ranging from 5000 to 4,440,000, the latter being the maximum test value attained.[1] This upper limit would include practically all truss bridges.

The curve of C_D vs R for circular disks is almost identical in shape to that for a rectangular plate in the critical range below an R-value of approximately 5000 (see Prof. Farquharson's Figure 1). It is more than probable that the two curves would be similar throughout and that the drag coefficient would be constant above this critical range.

The major drag producing components in a truss bridge are the truss members. It is logical to assume that the Reynolds' Number effect on these sharp-edged elements would be the same as on flat plates rather than being similar to the circular cylinder cited by Prof. Farquharson. It may therefore be concluded that test data on model trusses may be applied to full scale structures. The suggested test program on actual structural elements would be desirable, however, as further verification of this conclusion.

One of the conclusions in the paper under discussion stated that it was apparently unnecessary to construct models that included minute details of fabrication. This conclusion was reinforced by a series of

*Asst. Prof. of Structural Eng., Massachusetts Inst. of Technology, Cambridge, Mass.

1. James M. Shoemaker, National Advisory Committee for Aeronautics, Technical Note No. 252 (1926).

tests conducted by Mr. Abraham Perera in the M.I.T. Wind Tunnel.[2]

Mr. Perera constructed and tested truss models cut from plywood of various thicknesses. These models represented only a single truss and were identical in elevation to the brass truss shown in Fig. 2. The elevation area upon which the drag coefficient is based was the same for both plywood and brass models but the members of the plywood models were of solid rectangular cross-section and contained no structural details whatsoever. The results obtained were indicated in Table I.

TABLE I

Model	Drag Coefficient $\alpha = 0$
Brass Truss (See Fig. 2.)	1.63
Plywood Truss 3/8" Thick	1.65
" " 1/2" Thick	1.60
" " 5/8" "	1.63
" " 3/4" "	1.50
" " 1 " "	1.45

Table I indicates that accurate drag coefficients for a single truss can be obtained using models having no structural details and simulating only the outlines of the truss members. The thickness of the members of the brass truss was 5/8" —this dimension being consistent with the scale of the model. Plywood models of this thickness or less gave very good results but larger thicknesses produced somewhat smaller coefficients. The conclusion implied is that the thickness of the model should be approximately to scale but the results are not particularly sensitive to this dimension.

The total load on the entire structure is given by the equation:

$$H = (C_A A_T)\, C_D \rho \frac{V^2}{2}$$

The coefficient C_A for which curves have been given (see Figs. 7-10) is not appreciably affected by the type of truss. The nature of the truss as reflected in the coefficient C_D is the predominate influence on the total load. These tests on simple plywood models indicate that C_D for a particular truss type may be determined very simply and inexpensively. By this procedure, the difficulties in the experimental determination of wind loads on a complete bridge may be greatly reduced.

2. "Wind-Tunnel Testing of Simplified Bridge Truss Models" M.I.T. Thesis (B.S.), January, 1954.

DISCUSSION OF THE AMPLIFICATION OF
STRESS IN FLEXIBLE STEEL ARCHES
PROCEEDINGS-SEPARATE NO. 245

ROBERT S. ROWE,* A.M. ASCE.—The discussion by Mile S. Ketchum adds materially to the paper in presenting additional evidence in comparing the results of the amplification of stress by a simplified and more precise method. The author agrees with Mr. Ketchum that the use of the amplification chart should be very helpful in making a preliminary estimate of the amplification of stress in steel arches, especially for problems where time-consuming studies may be indicated.

---

*Associate Prof., Dept. of Civ. Eng., Princeton Univ., Princeton, N. J.

DISCUSSION OF LATERAL BUCKLING OF I BEAMS UNDER THRUST AND UNEQUAL END MOMENTS PROCEEDINGS-SEPARATE NO. 291

ROBERT V. WHITMAN,* J.M. ASCE.—**At approximately the time when the studies described in this paper were carried out, the writer also undertook a brief investigation of the lateral buckling of simply supported single span beams loaded by axial thrust and unequal end movements.[1] The method of Stodola and Vianello was used in these studies with the deflections u and β represented by two or in some cases three terms of sine series. The solutions, although not carried out with as much accuracy as those obtained by the author and for but two values of the ℓ^2/a^2 parameter, are in substantial agreement with the author's results and thus afford a gratifying check.**

The eleven graphs presented by the author can effectively be combined into a single graph by using a generalization of the author's equation 1. In Figure A the author's results have been replotted using the ratio M/M_{cr} for the abscissa, where now M_{cr} is the critical value of M_2 when no axial thrust is present. The portions of the curves for r = -0.8 shown dotted could not be determined directly from the author's solutions and their trend is based upon numerical values obtained by the writer during his investigations. Equation 1, represented by the curve for r = 1, is a parobola and as shown by Johnston(2) is independent of the value of the parameter ℓ^2/a^2. The interaction curve for r = 0.5 differs by so little from that for r = 1 that the difference does not appear on the graph, and even for r = 0 the position of the interaction curve has shifted only slightly. Moreover, for values of r down to -0.8 variations of the parameter ℓ^2/a^2 from 0.1 to infinity cause only small shifts in the interaction curve positions. In fact the interaction curves for values of ℓ^2/a^2 between 0.1 and 100 are so identical that their differences could not be shown on the graph. It is only when r approaches -1 that differences in ℓ^2/a^2 cause significant changes in the interaction curves.

This composite set of curves shows in a clear manner the effect of unequal end moments upon the shape of the interaction curve. It should be of considerable practical interest to know that the curves for values of r between one and zero differ by so little, and that the effect of the parameter ℓ^2/a^2 is generally small.

***Assistant Prof. of Soil Mechanics, Massachusetts Inst. of Technology, Cambridge, Mass.**

1. Whitman, R. V., "Flexural - Torsional Buckling of Eccentrically Loaded Columns", submitted in partial fulfillment of the requirements for the degree of Doctor of Science, Massachusetts Institute of Technology, September 1951 (Unpublished).

The conditions which lead to the sharp breaks in the interaction curves for $r = -1$ are worthy of further comment. The two branches of the curves represent two different modes of buckling. The branches running along the top part of the graph correspond to solutions in which the deflection u is symmetrical with respect to midspan and the rotation β is antisymmetrical. The reverse conditions are present in the solutions represented by the branches ascending along the left side of the graph. As might be expected the solution with u symmetrical is critical when thrust is more predominant than bending, with the reverse condition when the bending movements are predominant. If the ascending branch of the interaction curve for $r = -1$ were to be extended to value greater than $P/P_{cr} = 1$, it would meet the vertical axis at $P/P_{cr} = 4$, corresponding to second mode of the Euler buckling condition.

MICHAEL R. HORNE,*.—The author quotes an expression (equation (1)) for critical combinations of end thrust P and equal end moments M as obtained by Timoshenko and Johnston. This solution does not allow for the reduction of torsional rigidity due to end thrust. The complete solution (Bleich[7], Goodier[8] and Hall and Clark[10]) is, in terms of the author's notation,

$$K^2 = \pi^2 \left\{ 1 - \frac{P}{P_E} \right\} \left\{ 1 + \frac{\frac{\pi^2 a^2}{\ell^2}}{\left(1 - \frac{PI_p}{AC}\right)} \right\} \tag{29}$$

The results given by Professor Salvadori for the case $r = 1$ should agree with this equation. It will however be seen that K cannot be expressed as a function of $p \left(= \frac{P}{P_e}\right)$ and $\frac{\ell^2}{a^2}$, since the term $\left(1 - \frac{PI_p}{AC}\right)$ is involved. Investigation of Professor Salvadori's Tables shows that he has assumed the term $\left(1 - \frac{PI_p}{AC}\right)$ to be equal to unity. Since the same term occurs in the interpretation of the symbol K, and is not there assumed to have unit value, the treatment is illogical, although it does give an answer on the safe side. Results deduced from the Tables will therefore only be "accurate" provided $\frac{PI_p}{AC}$ is small compared with unity, or when $\frac{\ell^2}{a^2}$ is large compared with π^2.

It is possible to obtain an approximate expression for critical combinations of axial load and unequal end moments, thus avoiding the use of extensive Tables. It follows from a paper by Worthington[11] that, if M_{cr} is the critical value of the larger end moment when the axial load is zero, and P_e is the Euler load for failure about the minor axis, then the following formula gives safe combinations of M_2 and P.

*Department of Engineering, University of Cambridge.

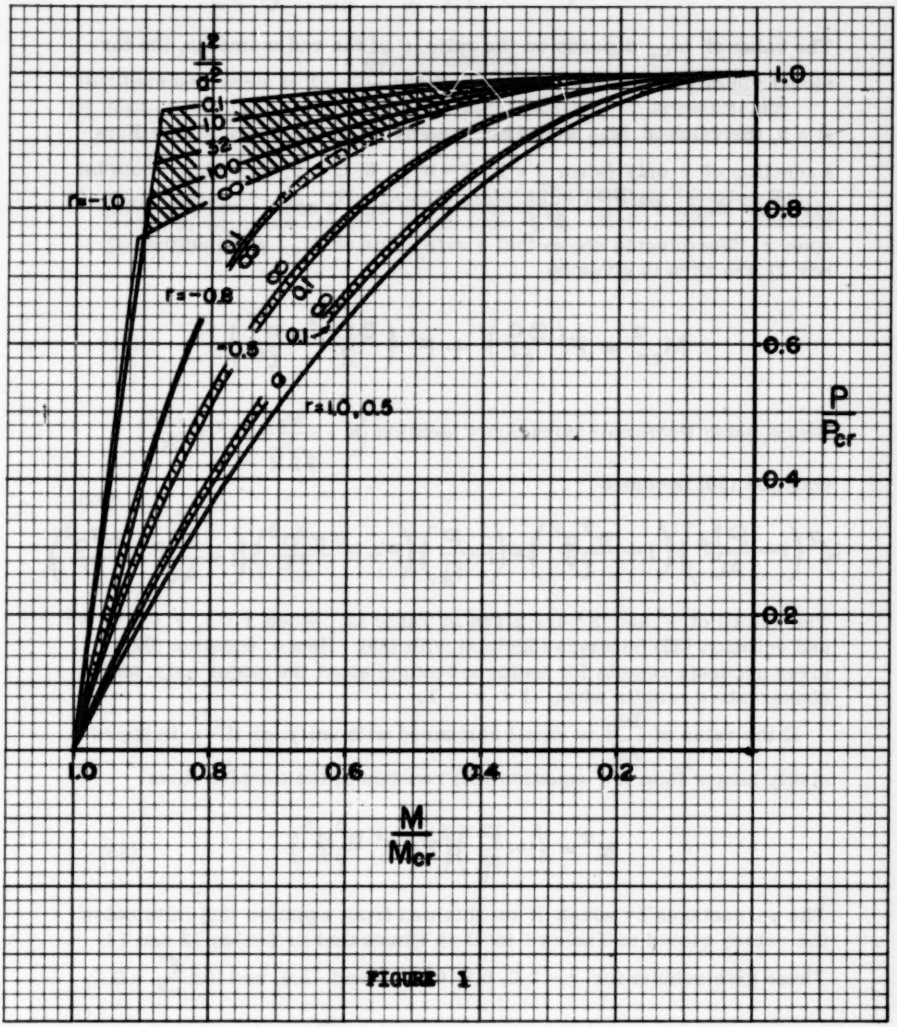

$\frac{l^2}{a^2}$
0.1
1.0
32
100
∞
r=-1.0
r=-0.8
-0.5
0
0.1
r=1.0, 0.5
1.0
0.8
0.6
0.4
0.2
$\frac{P}{P_{cr}}$
1.0
0.8
0.6
0.4
0.2
$\frac{M}{M_{cr}}$

FIGURE 1

$$\left(\frac{M_2}{M_{cr}}\right)^2 = \left\{1 - \frac{P}{P_E}\right\}\left\{1 - \frac{\frac{PI_p}{AC}}{\left(1 + \frac{Dh^2}{2C}\frac{\pi^2}{\ell^2}\right)}\right\} \tag{30}$$

The value of M_{cr} depends on the ratio r of the end moments, the torsional rigidity C and the warping rigidity $\frac{DL^2}{2}$. If it were assumed that $D = 0$, the value of M_{cr} would be given by $M_{cr}^2 = F\left(\frac{BC}{\ell^2}\right)$ where F is a function of r only (when $r = 1$, $F = \pi^2$). If $C = 0$, then M_{cr} would be given by $M_{cr}^2 = F^1\left(\frac{BDh^2}{2}\frac{\pi^2}{\ell^4}\right)$ where F^1 is also a coefficient depending upon r. Worthington shows that a safe value of M_{cr} when neither C nor D are zero is given by

$$M_{cr}^2 = F\left(\frac{BC}{\ell^2}\right) + F'\left(\frac{BDh^2}{2}\frac{\pi^2}{\ell^4}\right) \tag{31}$$

Hence, using Professor Salvadori's notation $\left(K = \frac{M_2\ell}{\sqrt{BH}},\ a^2 = \frac{Dh^2}{2C}\right)$ equation (30) becomes

$$K^2\left(1 - \frac{PI_p}{AC}\right)\left(1 + \frac{\pi^2 a^2}{\ell^2}\right) = \left(1 - \frac{P}{P_E}\right)\left(F + F'\frac{\pi^2 a^2}{\ell^2}\right)\left(1 - \frac{PI_p}{AC} + \frac{\pi^2 a^2}{\ell^2}\right) \tag{32}$$

The values of F and F^1 are given in Table 12. When $r = 1$, $F = F^1 = \pi^2$ and equation (32) becomes identical with (29). Hence, equation (32) gives accurate results for uniform bending about the major axis, and conservative results when $-1 < r < 1$.

If the value of $\frac{PI_p}{AC}$ is small compared with unity, or if $\frac{\ell^2}{a^2}$ is appreciably larger than π^2, equation (32) reduces to the simpler form

$$K^2 = \left(1 - \frac{P}{P_E}\right)\left(F + F'\frac{\pi^2 a^2}{\ell^2}\right) \tag{33}$$

The percentages by which K as obtained from equation (33) falls below the values quoted in Tables 1 to 11 is illustrated in Tables 13 and 14. These give results for $r = 1.0, 0.5, 0, -0.5$ and -1.0, and for $\frac{\ell^2}{a^2} = 0.1$, 1.0, 10, 100 and ∞. Table 13 corresponds to $\frac{P}{P_e} = 0$ and Table 14 to $\frac{P}{P_e} = 0.6$. Results are quoted to the nearest half percent. It will be seen that the approximate formula gives results sufficiently accurate

for practical purposes when the value of r is positive, but not when it is negative. This is due to the fact that the fundamental modes of lateral deflection when bending moments act alone and when axial load acts alone respectively are similar when r is positive, but become increasingly dissimilar as r approaches -1.

REFERENCES

10. Hall, H. N. and Clark, J. W. "Laterial Buckling of Eccentrically Loaded I-Section Columns". Trans. A.S.C.E. Vol. 116 (1951), p. 1179.

11. Worthington, P. M. "The Elastic Stability of Straight I-beams Subjected to Complex Loads". Proc. Inst. C. E. Part I. Vol. 3 (January 1954), p. 46.

r	F	F'
1.0	9.87	9.87
0.9	10.96	11.44
0.8	12.11	12.78
0.7	13.54	14.10
0.6	15.13	15.50
0.5	16.97	17.16
0.4	19.10	19.22
0.3	21.53	21.82
0.2	24.30	25.10
0.1	27.46	29.14
0	30.9	34.0
- 0.1	34.8	39.8
- 0.2	39.1	44.3
- 0.3	43.7	53.4
- 0.4	48.6	60.8
- 0.5	53.6	67.9
- 0.6	58.7	74.3
- 0.7	63.4	78.9
- 0.8	67.1	81.0
- 0.9	68.1	79.7
- 1.	64.5	74.1

Table 12

Values of the constants F and F' in equations (32) and (33)

$$\frac{P}{P_E} = 0$$

r \ $\frac{l^2}{a^2}$	0.1	1.0	10	100	∞
1.0	0	0	0	0	0
0.5	0	0	0	0	0
0	0.5	0.5	1.5	1.5	0
- 0.5	0.5	1.0	3.5	3.0	0
- 1.0	0	0.5	3.0	1.5	0

Table 13

$$\frac{P}{P_E} = 0.6$$

r \ $\frac{l^2}{a^2}$	0.1	1.0	10	100	∞
1.0	0	0	0	0	0
0.5	0.5	0.5	0.5	0.5	0.5
0	3.5	4.0	5.0	6.0	5.5
- 0.5	15.5	16.0	18.5	18.5	17.0
- 1.0	31.5	32.0	33.5	32.5	31.5

Table 14

Percentages by which K estimated from equation (33) falls below results given by Salvadori.

MARIO G. SALVADORI,* M. ASCE.—The form of interaction curves suggested by Mr. Whitman is very illuminating. It not only allows a more concise graphical presentation of the writer's results, but indicates the important physical fact that for values of the ratio r between zero and one, the interaction curves are insensitive to the values of the parameter ℓ^2/a^2.

In a paper currently in preparation, the writer plans to present in this form additional interaction curves for conditions of support other than "simple support" in the weaker plane. Of course, the graphs of Mr. Whitman must be used in connection with a table of critical values of M_2 for p = 0, which should appear, possibly, in a corner of the graphical presentation.

The results obtained, in an approximate fashion by Mr. Horne do not seem to be of interest for the following reasons:

1) The advantage of a concise presentation is available in connection with accurate results as soon as the writer's curves are combined as suggested by Mr. Whitman.
2) The approximate results obtained by Mr. Horne are much too conservative as soon as r is less than zero, as shown by his computations.
3) The weakening of the beam due to pure torsional buckling under thrust is of no practical importance, since the critical thrust for pure torsional buckling is very high for the type of beams to which the writer's results are to be applied in design. Moreover, Mr. Horne is referred to the statement by the writer indicating how to obtain in a very simple manner a more accurate value of the critical moment, i.e., of the factor K, in those rare cases in which torsional buckling becomes significant. Such statement appears in the third paragraph on p. 6 of the Separate.

CORRECTIONS FOR TRANSACTIONS.—In Eq. 1, the first term should not be squared, the correct expression being as follows:

$$\frac{P}{P_{cr}} + \left(\frac{M}{M_{cr}}\right)^2 = 1 \qquad (1)$$

*Prof. of Civ. Eng., Columbia Univ., New York, N.Y.